Available online at www.sciencedirect.com

ScienceDirect

Procedia CIRP 101 (2021) 250–253

www.elsevier.com/locate/procedia

9th CIRP Conference on High Performance Cutting (HPC 2020)

Evaluating tool point dynamics using smartphone-based visual vibrometry

Pulkit Gupta[a], Mohit Law[a,*]

[a]*Machine Tool Dynamics Laboratory, Department of Mechanical Engineering, Indian Institute of Technology Kanpur, Kanpur 208016, India*

* Corresponding author. Tel.: +91-512-679-6897; fax: +91-512-679-7408. *E-mail address:* mlaw@iitk.ac.in

Abstract

Modern smartphones can record high megapixel videos at high frame rates. This paper leverages these capabilities and presents a new method to evaluate dynamics of a representative grooving tool using a smartphone's video camera. Pixels within images are treated as vibration sensors measuring response to impact-based excitation. Motion is detected and tracked using image processing techniques to give pixel-displacement time series data. Spectra of these data give natural frequencies, and damping is estimated using the logarithmic decrement method. These parameters compare well with those extracted using experimental modal analysis procedures. Unscaled tool vibration shapes are visualized using motion magnification techniques.

Keywords: Cutting tool; Dynamics; Visual vibrometry

1. Introduction

Knowledge of the dynamics of the machine, the cutting tool, and the flexible workpiece are essential to guide the selection of chatter-free cutting parameters [1]. Accurately measuring these dynamics remains difficult [2], and hence is of great interest and concern to the machine tool community.

The conventional method to measure dynamics involves the use of experimental modal analysis (EMA) procedures. These procedures use a modal impact hammer or a modal shaker to excite the system, and the resulting response is usually measured using accelerometers. Modal parameters such as the natural frequency, damping, and shapes are determined using one of the many time or frequency domain system identification techniques [3]. Though these procedures are straightforward, and are often used by practitioners and researchers, sometimes, the added mass of the accelerometer can corrupt the measured dynamics. Though the use of non-contact eddy-current sensors and laser Doppler vibrometers (LDV) can avoid any potential mass-loading issues, LDVs are expensive, and eddy-current sensors can be difficult to calibrate and instrument.

To address these issues, this paper proposes a new use of a video camera-based vibration measurement technique referred to as visual vibrometry – for machine tool applications. Visual vibrometry methods track displacements in videos by monitoring the pixel-intensity variations across frames using well-established image correlation and processing techniques. Moreover, since these methods do not need dedicated data acquisition systems and rely only on using a camera with some post-processing of video, these methods are increasingly being used in modal analysis and structural health monitoring of civil infrastructure [4-7]. Though these methods are effective, their use is constrained by how expensive high frame rate cameras are. Given the ubiquity of inexpensive modern smartphone cameras and that these cameras can record high megapixel videos at high frame rates, these cameras are also increasingly being used in the vibration monitoring of bridges [8], beams [9], and other civil infrastructure [10].

Building on the successful use of visual vibrometry in other engineering domains, this paper demonstrates its use for evaluating the dynamics of a representative cutting tool. We leverage the capabilities of a typical modern and inexpensive

10.1016/j.procir.2020.09.196

smartphone camera to record video of the vibrating tool and use established methods to detect and track the vibrating edge of the tool to extract its displacement. Though some modern smartphones can record videos at 960 frames per second (fps), we use a camera that can sample up to 480 fps. The test setup is described in Section 2, and edge detection and tracking are discussed in Section 3. We deliberately design a test setup of the tool such that the tool behaves like a single degree of freedom system such that we can use a simple spectral method and the logarithmic decrement method to estimate the natural frequency and damping, respectively. This modal parameter extraction is discussed in Section 4. Section 4 also benchmarks visual vibrometry results with results obtained using conventional EMA procedures. Shape analysis, which is greatly aided by vision-based methods is discussed in Section 5, following which, the paper is concluded.

2. Experimental setup

The experimental setup consists of a grooving blade with a width of 7.5 mm and an overhang of 200 mm secured in a holder mounted on machine bed as shown in Fig. 1. The setup was designed such that the response of the blade is akin to the response of a single degree of freedom system. The overhang was chosen such that the dominant mode can be captured by the maximum frame rate available on the smartphone camera. The setups, as shown in Fig. 1(a-b) facilitated separate measurements using an accelerometer, an eddy-current sensor, and a OnePlus 7t smartphone-camera to record the response. In the case of the accelerometer and the eddy-current sensor, the data was recorded with a National Instruments' (NI) data acquisition system (NI9234 + NI9171) using CutPro®'s modal analysis module. Acquired data for these sensors were sampled at 51.2 kHz, whereas smartphone-based measurements were recorded at a sampling rate of 480 frames per second (fps). The resolution of camera-based measurement was 720 x 1280 with a field of view of 27 mm x 48 mm, resulting in a per-pixel resolution of 37.5 µm. The distance between the tool and the camera was 100 mm, whereas the distance between the tool and eddy-current sensor was 600 µm.

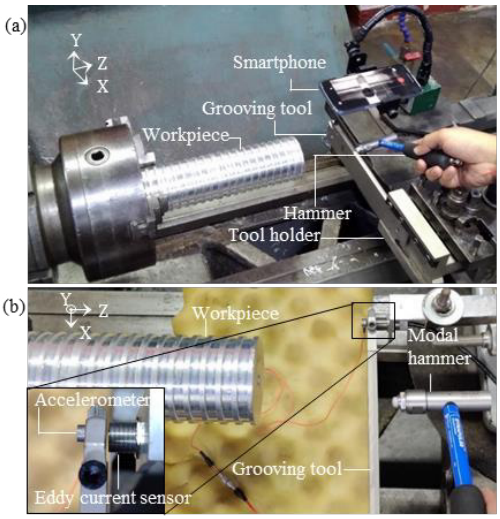

Figure 1. Experimental setup (a) smartphone-camera aided vision-based vibration measurement; (b) conventional EMA with an accelerometer and an eddy-current sensor.

Camera measurements required a white screen which was kept as a monotone background under the grooving blade setup. Only in-plane response can be measured and separate measurements or a stereo setup is required for response in different directions. The blade was excited using a modal hammer for all measurements. Since it is difficult to synchronize the video recording to the input excitation, visual vibrometry is generally an output-only modal analysis method, and, as such, all inputs in this study also remain unmeasured. Video was recorded for ~5 seconds and saved in the MP4 format. Individual frames of the video were processed in MATLAB R2018b to detect and track the response of the edge(s) – as discussed next.

3. Extracting displacements by tracking the detected edge

This section first describes the procedure to detect the edge followed by discussions on extracting displacements from the tracked edge.

3.1. Edge detection

To detect edges of the vibrating object, we prefer to use the Canny edge detector [11], which is simpler to implement than other digital image correlation or optical flow techniques [4-7]. The aim is to detect the vibrating edge of the grooving tool around the cutting region, i.e., at the free end of the blade. The Canny edge detection procedure involves five key steps that are summarized below. Edge detection involves computation of image gradients and therefore, it is sensitive to image noise.

Since the image may be noisy, the first step deals with noise reduction and involves convolving the image with a Gaussian blur to smoothen it. The Gaussian kernel of variance, σ^2 and size, $(2n+1)\times(2n+1)$ is given in Eq. (1):

$$G_{ij} = \frac{1}{2\pi\sigma^2}\exp\left(-\frac{(i-n-1)^2+(j-n-1)^2}{2\sigma^2}\right) \quad 1 \le i,j \le (2n+1). \tag{1}$$

wherein i, j correspond to the pixel of interest. In the present implementation, the variance and size are: $\sigma^2 = 2$ and $n = 5$.

Since the edge is defined by a change in the pixels' intensity value, i.e., edge detection involves computation of image gradients, the second step involves taking image derivatives, $\mathbf{I_x}$ and $\mathbf{I_y}$ which are calculated to compute the change in intensity by convolving with Sobel kernels, $\mathbf{S_x}$ and $\mathbf{S_y}$ that are given in Eq. (2). The magnitude and slope for the gradient are given in Eq. (3).

$$\mathbf{S_x} = \begin{pmatrix} -1 & 0 & 1 \\ -2 & 0 & 2 \\ -1 & 0 & 1 \end{pmatrix}, \mathbf{S_y} = \begin{pmatrix} 1 & 2 & 1 \\ 0 & 0 & 0 \\ -1 & -2 & -1 \end{pmatrix}. \tag{2}$$

$$|\mathbf{M}| = \sqrt{\mathbf{I_x^2} + \mathbf{I_y^2}}, \mathbf{\Theta} = \arctan\left(\mathbf{I_x}/\mathbf{I_y}\right). \tag{3}$$

Since thick and thin edges can both be present, the third step addresses this issue by storing only the maximum intensity value from the intensity gradient matrix, $|\mathbf{M}|$ along the edge direction, $\mathbf{\Theta}$. Even after this, some edges tend to be brighter than others, and this is addressed in the fourth step.

The problem of differential brightness in the detected edges is addressed by using a double threshold. The higher threshold is used to identify edges with high-intensity values whereas the lower threshold identifies non-relevant low-intensity pixels and discards them. If there happen to be pixels with intensities in between the two thresholds, then the fifth and final step involves converting low-intensity pixels into higher ones if at least one of the pixels in the neighbourhood of the one being processed is a high-intensity pixel. This procedure results in a binary frame comprising edge information which is represented by ones and zero otherwise. The detected edge for a frame is shown in Fig. 2. For illustration purposes, the grooving tool is oriented in horizontal direction. The above procedure is repeated for all frames of interest to then extract displacements – as is discussed next.

3.2. Tracking the edge across frames to extract displacements

The procedure to track the edge(s) across frames and to extract displacement from the tracked edge is as follows: each frame was traversed along the columns in the entire range of rows and the location of the first occurrence of binary 'one' was stored as the instantaneous edge position for that frame. This was done for all the frames. This procedure is schematically also shown in Fig. 2. Although every pixel is a sensor, we averaged the motion of 10 pixels around the tip of the tool to better capture motion. The resulting response was mean centred – as is evident also in Fig. 2.

Since edge detection and subsequent tracking is thought to be a function of the threshold limits within the edge detection algorithm, Fig. 2 also shows the sensitivity of the extracted response to changing thresholds. Fig. 2 specifies only the upper threshold limit. The lower threshold limit was taken to be 0.4 times the upper threshold limit in every case. As is amply evident, the acquired response is seemingly independent of the threshold limit. The displacements thus extracted are processed to obtain the modal parameters of interest – as is discussed next.

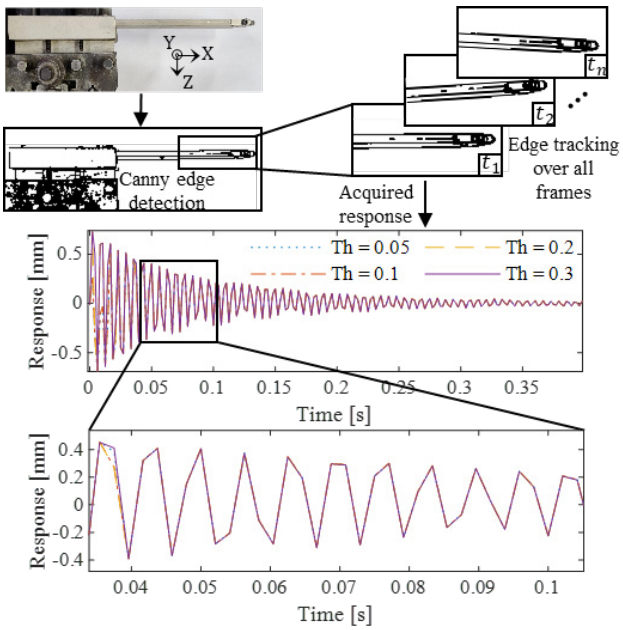

Figure 2. Schematic overview of edge detection and tracking, and comparison of extracted response for different threshold (Th) limits.

4. Modal parameter extraction from measured response

Damping is estimated using the logarithmic decrement method [3] and the natural frequency is estimated from the frequency spectra of the measured response. The measured time series data extracted using visual vibrometry is compared in Fig. 3 with the response measured using the eddy-current sensor and the accelerometer. The accelerometer signal was twice integrated to obtain displacements. As is evident from Fig. 3, the response with all three methods is in very close agreement with each other. Smartphone-camera based measurement was sampled at 480 fps whereas measurements with the other sensors were sampled at 51.2 kHz, and hence the acquired response signal in Fig. 3 for the other sensors is a lot smoother as compared to the discrete looking points joined together in the case of the measurement with the smartphone. Nevertheless, the damping estimated from this response compares rather well with the damping estimates from the measured response of the eddy-current sensor and the accelerometer. Damping comparisons are tabulated in Table 1.

Table 1 also lists the natural frequencies estimated from the spectra of the response signals shown in Fig. 4. Again, because of the sparser nature of the vision-based response measurement, the peak in the spectra is weaker in comparison to the peaks in the spectra of the eddy-current sensor signal and the accelerometer signal. Despite the peak being weaker for the measurement with the smartphone camera, the natural frequency estimates for all three methods are in very good agreement with each other – as is evident from Table 1.

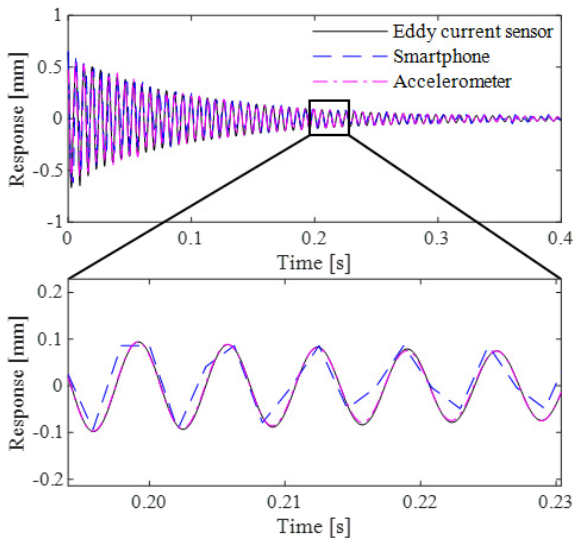

Figure 3. Comparison of measured response with three different methods.

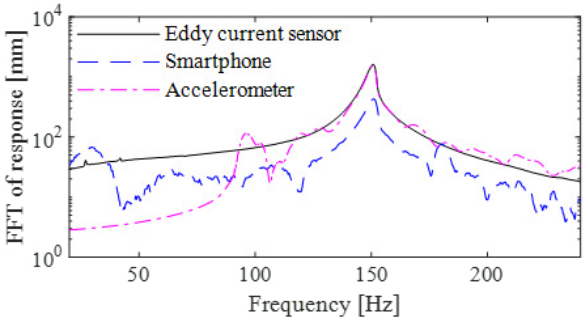

Figure 4. Comparison of frequency spectra of three different measurements.

Table 1.
Comparison of extracted modal parameters of the grooving tool for three different measurement methods.

	Natural frequency	Damping ratio
Accelerometer	150.7 Hz	1.08 %
Eddy current sensor	150.8 Hz	1.08 %
Visual vibrometry	150.8 Hz	1.11 %

5. Mode shape visualization

One of the main advantages of visual vibrometry is that full-field mode shape analysis is much simple than it would be using the conventional EMA methods with roving/scanning sensors or hammers. However, since motion is typically small, phase-based motion magnification techniques [7] are used herein to amplify movement. Phase-based motion magnification involves small movements in videos being processed in complex-valued image pyramids. Complex steerable pyramid [12] is a transform that decomposes an image according to spatial scale, orientation, and position. Variations in the phase of complex-valued steerable pyramids represent the motion over time. This motion is then amplified for better visualization of imperceptible motion.

Implementation of the motion magnification technique proceeds as follows: at first, the amplitude of local wavelets is separated from their phase with the complex steerable pyramids. This is followed by temporally band-passing decomposed phases independently at each location, orientation and scale in the frequency domain. Amplitude-weighted spatial smoothing is then performed to improve the phase signal-to-noise ratio, followed by amplification or attenuation of temporally band-passed phases. The video is reconstructed from the resulting phase and amplitude wavelets.

Above procedure was applied to separate far-field video recordings of the grooving tool setup at 480 fps. The distance of the smartphone camera for the far-filed recordings was increased to be 400 mm from the setup. The field of view was 320 mm x 180 mm with a per-pixel density of 0.25 mm/px. Since the mode is at 150.8 Hz, the video was band-passed between 148 Hz and 152 Hz, respectively. The motion amplification factor was set to 100% and the noise attenuation factor was set to 20%. The resulting video displayed a motion like that of the fundamental mode of a cantilever beam, and a representative illustration of when the motion is largest is shown in Fig. 5, which is overlaid on the undeformed configuration of the tool. This full-filed mode shape visualization using visual vibrometry can be compared to the traditional method of obtaining shapes by roving the sensor and/or the hammer (actuator), as was illustrated in [13].

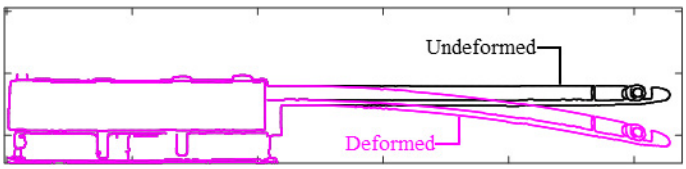

Figure 5. Phase-based motion magnified mode shape of the grooving tool.

6. Conclusions and outlook

This paper demonstrated the use of visual vibrometry – a vision-based vibration measurement technique, to evaluate the dynamics of a representative cutting tool. Capabilities of modern smartphones to record high megapixel videos being recorded at high frame rates were leveraged to extract the modal parameters of interest. Modal parameters thus extracted were found to compare well with parameters extracted with other accelerometer and eddy-current sensors. Full shape visualization was demonstrated to be easier with motion magnification techniques.

Though results demonstrated herein were for a tool whose response was dominated by a single low-frequency mode such that it was identifiable using the camera recording video at 480 fps, methods presented are generalizable, and can be used for multi-mode analysis. Furthermore, methods presented may also be extended to evaluating the dynamics of other tools such as end mills vibrating at higher frequencies, as long as the smartphone can record video at frames rates higher than at least twice the natural frequencies of the tools of interest, i.e., if sampling respects the Nyquist criterion. And, given the rapid developments in cameras on modern smartphones, and the progress in computer vision techniques, visual vibrometry has the potential to further facilitate vibration measurements of machine tool systems.

Acknowledgements

This work was partially supported by the Government of India's Impacting Research Innovation and Technology initiative through project number IMPRINT 5509.

References

[1] Okubo N, Yoshida Y, Hoshi T. Application of modal analysis to machine tool structures. *CIRP Annals* (1982); 31(1):243-246.
[2] Munoa J, et al. Chatter suppression techniques in metal cutting. *CIRP Annals* (2016); 65(2):785-808.
[3] Maia NMM, e Silva JMM. Theoretical and experimental modal analysis. *Research Studies Press* (1997).
[4] Xu Y, Brownjohn JMW. Review of machine-vision based methodologies for displacement measurement in civil structures. *J. of Civil SHM* (2018).
[5] Feng D, Feng MQ. Computer vision for SHM of civil infrastructure: From dynamic response measurement to damage detection–A review. *Engineering Structures* (2018); 156:105-117.
[6] Spencer Jr BF, et al. Advances in Computer Vision-Based Civil Infrastructure Inspection and Monitoring. *Engineering* (2019); 5(2).
[7] Chen J, et al. Modal identification of simple structures with high-speed video using motion magnification. *J. of Sound and Vibration* (2015); 345.
[8] Zhao X, et al. Experimental research on quick structural health monitoring technique for bridges using smartphone. *Advances in Materials Science and Engineering* (2016); 2016.
[9] Orak MS, Ozturk T. Monitoring cantilever beam with a vision-based algorithm and smartphone. *Vibroengineering PROCEDIA* (2018); 17.
[10] Kromanis R, et al. Measuring structural deformations in the laboratory environment using smartphones. *Frontiers in Built Environment* (2019).
[11] Canny, J. A Computational Approach to Edge Detection, *IEEE Transaction on Pattern Analysis and Machine Intelligence* (1986); 8(6).
[12] Portilla J, Simoncelli EP. A parametric texture model based on joint statistics of complex wavelet coefficients. *Intl. J. Comput Vision* (2000).
[13] Law M, et al. Modal analysis of machine tools using visual vibrometry and output-only methods. CIRP Annals, (2020); 69(1).